# Study on the Effect of Inorganic Fiber on the Energy Storage Characteristics of Sandwich Composite Films


**Yang Cui, Guang Liu, and Chang Hai Zhang**

**Abstract** Polymer-based composite dielectrics are expected to be widely used as key materials for thin film capacitors in fields such as pulsed power supplies and high-power energy storage systems due to their excellent breakdown performance and excellent flexibility. This work uses PVDF polymers as a matrix and introduces PMMA to reduce dielectric loss. Inorganic fibers with different structures were designed and filled into the intermediate layer of the sandwich structure, with polymers selected as outer layers on both sides to maintain flexibility. It was found that the addition of Ag particles can effectively improve the polarization strength of the composite film, but the breakdown characteristics also deteriorate. However, the addition of the $Al_2O_3$ shell layer can effectively alleviate the problem of breakdown degradation and reduce ferroelectric losses. Finally, ABA Film has the best energy storage characteristics, with a discharge energy storage density of 5.98 J/cm$^2$, and a charge–discharge efficiency of not less than 65.4%.

**Keywords** Core shell structure · Sandwich film · Energy storage density

## 1 Introduction

Dielectric capacitors exhibit advantages such as high voltage, extremely high power density, ultra-long service life, and high reliability, making them important in the fields of new energy, power transmission and transformation engineering, and electromagnetic weapons [1]. The energy storage density of dielectric capacitors is closely

Y. Cui (✉) · G. Liu
School of Electrical Engineering, Zhejiang University of Water Resources and Electric Power, Nanxun Campus, Hangzhou, China
e-mail: cuiy@zjweu.edu.cn

C. H. Zhang
School of Electrical and Electronic Engineering, Harbin University of Science and Technology, Harbin, China



S. Yadav et al. (eds.), *Energy Power and Automation Engineering*, Lecture Notes in Electrical Engineering 1118, https://doi.org/10.1007/978-981-99-8878-5_8

related to their dielectric constant ($\varepsilon_r$, polarization strength) and applied electric field ($E_b$, breakdown strength). Using high dielectric inorganic phase doping to improve the energy storage characteristics of polymer-based composite dielectrics is the most common method.

In the early days, researchers used high dielectric ferroelectric ceramic nanoparticles to increase the dielectric constant of composite dielectrics and improve their energy storage capacity. Dang et al. [2] found that the size of nanoparticles has an impact on the dielectric of composite dielectrics, which is related to interface polarization and the crystalline phase of nanoparticles. However, nanoparticles need to reach a certain amount of filling to significantly increase the dielectric constant, which can cause a serious decline in the dielectric breakdown strength. To alleviate the above problems, nanofibers were introduced into the polymer matrix. Zhang et al. [3] have found that nanofibers can generate large dipole moments, while their size advantage reduces the occurrence of agglomeration, which can effectively enhance the dielectric constant and energy storage density of composite dielectric. To achieve uniform filling phase dispersion and small electric field distortion, core–shell structured nanofibers have been extensively studied [4–8]. In addition, sandwich or multilayer structures have also been proven to maintain high breakdown strength [4]. The multi-layer structure design can not only adjust the electric field distribution in the dielectric at the macro-level but also combine the advantages of each layer [9], for example, using a composite dielectric containing 1 vol.% $BaTiO_3$ as the "hard layer" as the central layer to ensure high effective breakdown strength, and selecting a composite dielectric containing 10–50 vol.% $BaTiO_3$ as the "soft layer" for the outer layer to provide a high relative dielectric constant [4]. Based on the above research, it can be found that how to utilize the micro- and macro-interfaces is a key issue in improving the energy storage density of dielectric materials.

In this work, three types of inorganic fibers, namely single-phase inorganic fibers (BFs), two-phase doped inorganic fibers (BA Fs), and core–shell three-phase inorganic fibers (ABA Fs), were prepared and introduced into the intermediate layer of the sandwich structure. In addition, in order to alleviate the ferroelectric hysteresis loss of the PVDF matrix, a low-loss linear PMMA was blended with it to obtain a new polymer matrix. Based on this, three kinds of polymer-based sandwich structure films were prepared, and the influence of inorganic fiber structure on the energy storage characteristics of sandwich composite films was studied. It was found that the polarization intensity of the sandwich film filled with BA Fs was the highest under the same electric field, but the residual polarization was also large. Through the buffering of the shell layer, the applied electric field and residual polarization of the sandwich film have been positively improved, which enables the sandwich film to obtain a large energy storage density under a relatively higher electric field.

## 2 Experimental Section

### 2.1 Material

In this work, the ferroelectric polymer used is polyvinylidene fluoride produced by Shanghai Sannaifu New Material Technology Co., Ltd. The organic solvent used for dissolving polymers is N, N-dimethylformamide (DMF) produced by Chemical Reagents Co., Ltd. of China National Pharmaceutical Group. PMMA, $Al(NO_3)_3{\cdot}9H_2O$, $Ba(OH)_2{\cdot}8H_2O$, $Ca(OH)_2$, $C_{16}H_{36}O_4Ti$, $AgNO_3$, $NH_3{\cdot}H_2O$, $N_2H_4{\cdot}H_2O$, $C_2H_6O$, $CH_3$-COOH, $C_5H_8O_2$, and N, N-dimethylformamide (DMF) were purchased from Sinopharm Chemical Reagent Co. Ltd. $C_{20}H_{28}O_8Zr$, polyvinylpyrrolidone (PVP, K90), and tris(hydroxymethyl)aminomethane (tris) were purchased from Aladdin.

### 2.2 Preparation of Inorganic Filling Phase

The inorganic fibers used in this work include $Ba_{0.85}Ca_{0.15}Zr_{0.1}Ti_{0.9}O_3$ fiber (BCZT) abbreviated as B Fs, Ag particle doped B Fs abbreviated as BA Fs, and $Al_2O_3$ coated BA Fs core–shell fibers abbreviated as ABA Fs. The above inorganic fibers can be obtained by the method in previous work 1 [10].

### 2.3 Thin Film Preparation

The preparation methods of the PMMA/PVDF blend polymer layer and the inorganic fiber doped composite polymer layer prepared in this work can be obtained through the method in previous work 2 [11]. In this work, a blend polymer of 15% PMMA/PVDF was used as the outer layer in the sandwich structure. The composite polymer obtained by filling 3 vol.% inorganic fibers into a 15% PMMA/PVDF polymeric matrix serves as a sandwich intermediate layer. Finally, three thin films were successfully prepared, with 15% PMMA/PVDF-3 vol.% B Fs/15% PMMA/PVDF-15% PMMA/ PVDF abbreviated as B Film, 15% PMMA/PVDF-3 vol.% BA Fs/15% PMMA/PVDF-15% PMMA/PVDF abbreviated as BA Film, and 15% PMMA/PVDF-3 vol.% ABA Fs/15% PMMA/ PVDF-15% PMMA/PVDF abbreviated as ABA Film. The specific preparation process is shown in Fig. 1.

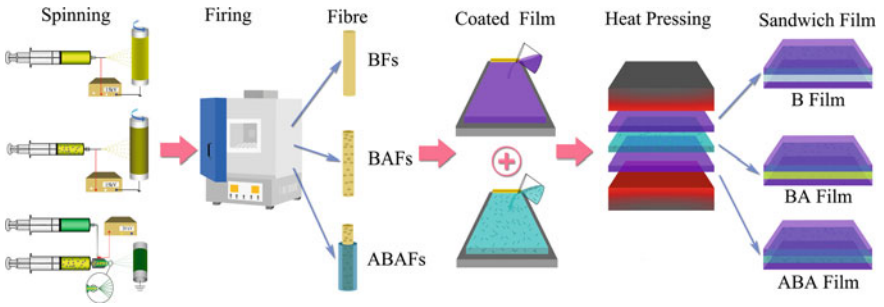


**Fig. 1** Flow chart of preparation of inorganic fibers and sandwich films

## 3 Results and Discussion

In this work, in order to determine the composite phase of the sandwich film prepared, it was first characterized by XRD, as shown in Fig. 2. As can be seen from the figure, an amorphous peak appeared at $2\theta = 15°–20°$ in the three thin films B Film, BA Film, and ABA Film, which was the characteristic peak formed after PMMA and PVDF were blended. The characteristic peak of $\theta = 20.1°$ is the PVDF characteristic peak [10, 11]. In addition, the characteristic peak of BCZT (indicated by the green dotted line) appeared in the three films, which is due to the BCZT phase contained in the inorganic fibers B Fs, BA Fs, and ABA Fs. The characteristic peak of Ag (indicated by the blue dotted line) appeared at $\theta = 38.1°$ in BA Film and ABA Film, and the characteristic peak of Ag in BA Film was stronger than that in ABA Film [11]. This is because the shell of ABA Fs is amorphous $Al_2O_3$ (indicated by the orange arrow), which weakens the characteristic peak of Ag. In addition to the above characteristic peaks, no other miscellaneous peaks were found, indicating that the polymer matrix and inorganic fiber phases were physically composite, and no chemical reaction occurred.

As a ferroelectric polymer, PVDF has a higher dielectric constant than ordinary polymers, but also a high dielectric loss, as shown in reference 11. In order to alleviate the problem of high loss, 15% PMMA was introduced into the polymer matrix in this work. From Fig. 3, it can be observed that due to the presence of intermediate inorganic fibers and the addition of multi-layer interfaces, the dielectric constant of sandwich structure composite films has not significantly decreased. The dielectric levels of the three thin films are basically consistent. However, the dielectric loss has been significantly suppressed due to the addition of PMMA, especially in the low-frequency region, which is basically less than 0.06 in the range of $10^0$–$10^5$ Hz. This is beneficial to the later suppression of hysteresis losses at high fields. In addition, due to the selection of pure polymers on both sides of the sandwich structure composite film, the overall conductivity basically remains at a relatively low level. From the above results, it is found that the structure of inorganic fibers has a relatively small impact on the polarization of sandwich composite films under low electric fields.

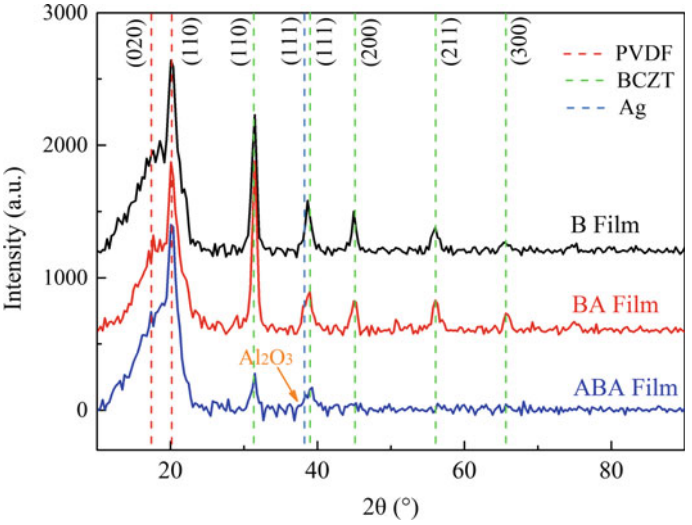


**Fig. 2** XRD patterns of sandwich films

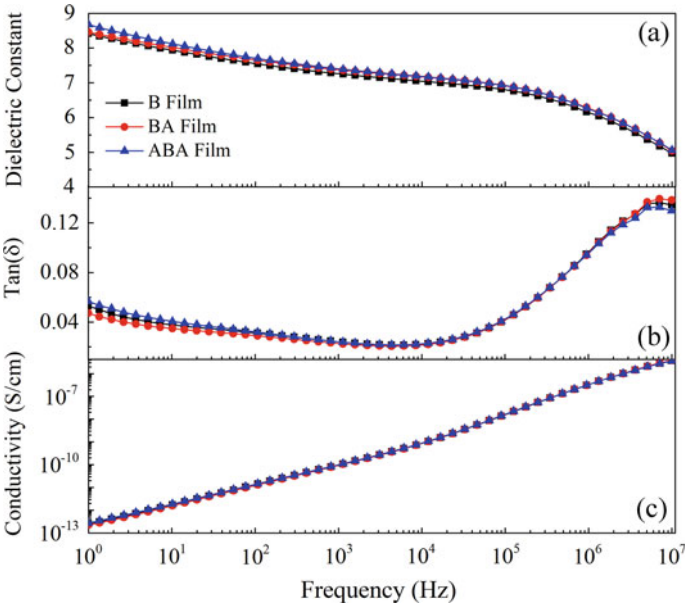


**Fig. 3** **a** Dielectric constant, **b** dielectric loss tangent, (c) conductivity of sandwich film

In order to better study the influence of inorganic fiber structure on the polarization and breakdown characteristics of sandwich composite films under high field conditions, D–E curve tests were conducted on three types of films: B Film, BA Film, and ABA Film, as shown in Fig. 4. From Fig. 4a, it can be seen that under the same electric field conditions, the film filled with BA Fs has the maximum polarization ($D_{max}$) and remnant polarization ($D_r$), due to the addition of conductive Ag. The film filled with ABA Fs having an $Al_2O_3$ shell layer has lower $D_{max}$ and $D_r$ than the film filled with BA Fs, where the composite film filled with B Fs has the smallest $D_{max}$ and $D_r$. This is due to the dielectric gradient effect of inorganic fiber structures. Wrapping a layer of $Al_2O_3$ with a dielectric constant similar to that of the matrix on the surface of high dielectric B Fs or BA Fs can reduce the MWS interfacial polarization in the composite. It is particularly worth noting that composite films with $Al_2O_3$ shells under the same conditions still have a lower $D_r$ when polarized at higher electric fields, which is beneficial to improving the breakdown strength of the composite films. This also means that once the electric field is removed, the stored energy can be more fully released [12, 13]. As shown in Fig. 4b, it is obvious that the addition of an inorganic fiber $Al_2O_3$ shell effectively enhances the breakdown strength of ABA Film, which makes it have the highest $D_{max}$.

In order to more clearly analyze the impact of inorganic fiber structure on polarization, Fig. 5 shows a comparison diagram of $D_{max}$ and $D_r$ under different electric fields. From Fig. 5a, b, it is found that in the entire electric field range, the $D_{max}$ and $D_r$ of BA Film are the highest, while the $D_{max}$ and $D_r$ of B Film are the lowest. And the $D_{max}$ and $D_r$ of each composite film increase with the increase of the electric field. $D_{max}$–$D_r$ is an important parameter representing the effective potential shift. As shown in Fig. 6, the $D_{max}$–$D_r$ of B Film is 2.21 μC/cm$^2$, with the addition of Ag particles, the $D_{max}$–$D_r$ of BA Film increases to 4.25 μC/cm$^2$. The addition of an $Al_2O_3$ shell further increases the $D_{max}$–$D_r$ value of ABA Film (4.56 μC/cm$^2$). According to the formula $D = \varepsilon_0\varepsilon_r E$, this may be due to the contributions of $\varepsilon_r$ and $E_b$. ABA Film has a relatively high $\varepsilon_r$ and $E_b$, resulting in the highest $D_{max}$–$D_r$, which is powerful for achieving high discharging energy density and charge–discharge efficiency.

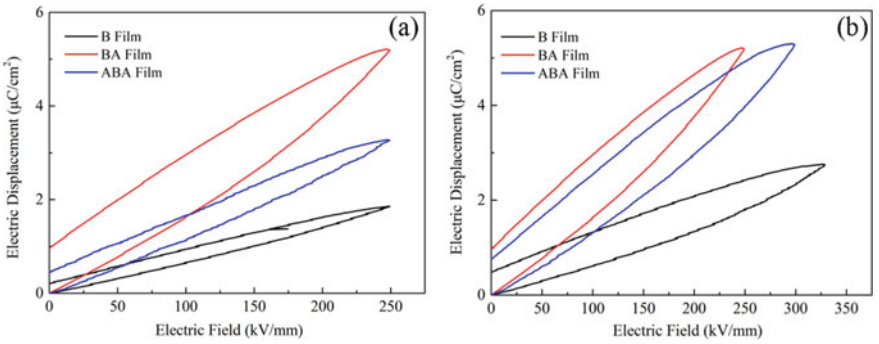


**Fig. 4** D-E curve of sandwich films. **a** At the same electric field, **b** at the maximum electric field

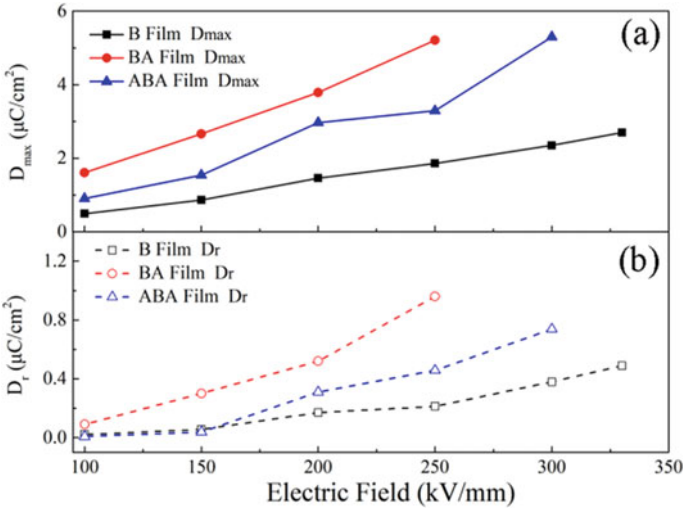


**Fig. 5** **a** $D_{max}$ and **b** $D_r$ curves under different electric fields

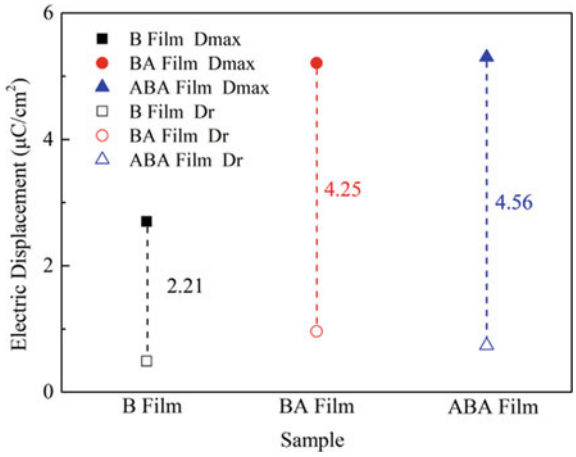


**Fig. 6** $D_{max}$–$D_r$ curves of sandwich films

The energy storage characteristics of the sandwich films are shown in the Fig. 7. Due to the advantage of $D_{max}$ of BA Film, it achieves the maximum charging energy density (7.36 J/cm$^2$) under the same electric field. However, excessive $D_r$ results in large energy loss, significantly weakening the advantage of discharging energy density (4.72 J/cm$^2$), and a sharp downward trend in charging–discharging efficiency. The breakdown electric field of B Film is the largest, but due to the minimum polarization intensity, its charging energy density (5.25 J/cm$^2$) and discharging energy density (3.25 J/cm$^2$) are both poor, but the charging–discharging efficiency has a relatively

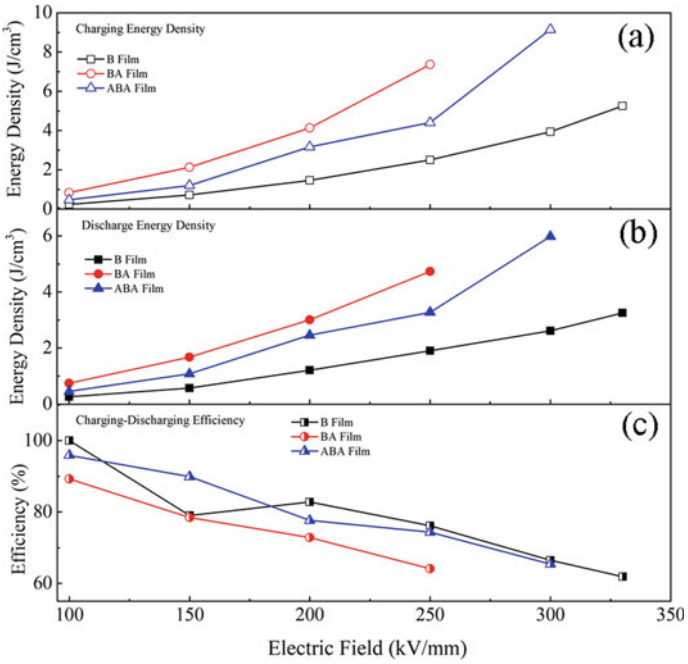


**Fig. 7** Energy storage characteristics of sandwich films. **a** Charging energy density, **b** discharge energy density, **c** charging–discharging efficiency

slow downward trend. Due to its relatively good breakdown electric field and polarization strength, ABA Film achieves the maximum charging energy density (9.14 J/cm$^2$) and discharging energy density (5.98 J/cm$^2$) under the maximum electric field, while the relative decline in charge–discharge efficiency is relatively flat, basically maintaining at 65.4% or above. Therefore, ABA Film has the best comprehensive energy storage characteristics.

## 4 Conclusion

In this work, three types of inorganic fibers were prepared and filled into the intermediate layer of the sandwich structure. The polymer matrix is selected as 15% PMMA/PVDF. The study found that the addition of Ag particles can effectively improve the polarization strength of BA Film, but at the same time cause a decrease in the breakdown field strength, resulting in a poor discharge energy storage density (4.72 J/cm$^2$). The addition of an $Al_2O_3$ shell layer effectively alleviated the breakdown field strength and ferroelectric losses of ABA Film, resulting in a discharge energy storage density of 5.98 J/cm$^2$ and a charge–discharge efficiency of no less than 65.4% for ABA Film.

**Acknowledgements** This research was supported by the Joint Funds of the Zhejiang Provincial Natural Science Foundation of China under Grant No. LZY22E030003, the National Natural Science Found at ion of China under Grant No.52007042, the Natural Science Foundation of Heilongjiang Province Joint Guide Project Grant LH2020E091. This research was supported by funded by the Nanxun Scholars Funding Program.

## References

1. Feng Q, Zhong S, Pei J, Zhao Y, Zhang D, Liu D, Zhang Y, Dang Z (2022) Chem Rev 122:3820–3878
2. Fan B, Zha J, Wang D, Zhao J, Dang Z (2012) Appl Phys Lett 100:2228
3. Zhang H, Marwat M, Xie B, Ashtar M, Liu K, Zhu Y, Zhang L, Fan P, Samart C, Ye Z (2019) ACS Appl Mater Interfaces 12:1–37
4. Luo H, Zhou X, Ellingford C, Zhang Y, Chen S, Zhou K, Zhang D, Bowen C, Wan C (2019) Chem Soc Rev 48:4424–4465
5. Guan L, Weng L, Zhang X, Wu Z, Li Q, Liu L (2020) J Mater Sci 55:15238–15251
6. Xu J, Fu C, Chu H, Wu X, Tan Z, Qian J, Li W, Song Z, Ran X, Nie W (2020) Sci Rep 10:17084
7. Rahimabady M, Mirshekarloo M, Yao K, Lu L (2013) Phys Chem Chem Phys 15:16242
8. Yang K, Huang X, He J, Jiang P (2015) Adv Mater Interfaces 2:1500361
9. Li H, Liu F, Fan B, Ai D, Peng Z, Wang Q (2018) Small Methods 2:1700399
10. Cui Y, Wang X, Zhang T, Zhang C, Chi Q (2019) RSC Adv B 33229–33237
11. Cui Y, Zhang T, Feng Y, Zhang C, Zhang Q, Zhang Y, Chen Q, Chen X, Lei Q (2019) Compos Part B Eng 177:107429
12. Xie Y, Jiang W, Fu T, Liu J, Zhang Z, Wang S (2018) ACS Appl Mater Interfaces 10:29038–29047
13. Pan Z, Yao L, Zhai J, Fu D, Shen B, Wang H (2017) ACS Appl Mater Interfaces 9:4024–4033